LEVEL

TRANSITION NOISE - THE ROLE OF FLUCTUATING
DISPLACEMENT THICKNESS

G. C. Lauchle

Technical Memorandum
File No. TM 80-41
27 March 1980
Contract No. N00024-79-C-6043

Copy No. 37

DTIC
ELECTE
JUN 4 1980
C

The Pennsylvania State University
Institute for Science and Engineering
APPLIED RESEARCH LABORATORY
Post Office Box 30
State College, PA 16801

NAVY DEPARTMENT

NAVAL SEA SYSTEMS COMMAND

Approved for Public Release
Distribution Unlimited

ADA 085103

80 6 3 024

REPORT DOCUMENTATION PAGE		READ INSTRUCTIONS BEFORE COMPLETING FORM
1. REPORT NUMBER TM 80-41	2. GOVT ACCESSION NO. AD-A085 103	3. RECIPIENT'S CATALOG NUMBER
4. TITLE (and Subtitle) TRANSITION NOISE - THE ROLE OF FLUCTUATING DISPLACEMENT THICKNESS		5. TYPE OF REPORT & PERIOD COVERED Technical Memorandum
		6. PERFORMING ORG. REPORT NUMBER
7. AUTHOR(s) G. C. Lauchle		8. CONTRACT OR GRANT NUMBER(s) N00024-79-C-6043
9. PERFORMING ORGANIZATION NAME AND ADDRESS Applied Research Laboratory P.O. Box 30 State College, PA 16801		10. PROGRAM ELEMENT, PROJECT, TASK AREA & WORK UNIT NUMBERS 39
11. CONTROLLING OFFICE NAME AND ADDRESS Naval Sea Systems Command Washington, DC 20362		12. REPORT DATE 27 March 1980
		13. NUMBER OF PAGES 32
14. MONITORING AGENCY NAME & ADDRESS(If different from Controlling Office) ARL/PSU/TM-80-41		15. SECURITY CLASS. (of this report) UNCLASSIFIED
		15a. DECLASSIFICATION DOWNGRADING SCHEDULE

16. DISTRIBUTION STATEMENT (of this Report)

Approved for Public Release. Distribution Unlimited.
Per NAVSEA - May 5, 1980.

17. DISTRIBUTION STATEMENT (of the abstract entered in Block 20, If different from Report)

18. SUPPLEMENTARY NOTES

19. KEY WORDS (Continue on reverse side if necessary and identify by block number)

boundary layer, displacement, fluctuating, turbulence

20. ABSTRACT (Continue on reverse side if necessary and identify by block number)

The role of the fluctuating wall shear stress on the noise generated by incompressible boundary-layer transition was recently analyzed [G. C. Lauchle, J. Acoust. Soc. Am. 67, 158-168 (1980)]. The solutions of that analysis suggest that the shear stress mechanism generates hydrodynamic sound weakly in comparison say to the sound generated by a fully developed turbulent boundary layer flow. Because boundary-layer transition is a very unstable and non-steady flow, we might expect that other acoustic mechanisms exist.

DD FORM 1473 EDITION OF 1 NOV 65 IS OBSOLETE
1 JAN 73

In this paper, we examine one other; namely, that of the fluctuating boundary
layer displacement thickness which is expected to occur as turbulent bursts
are created and convected over the surface. The snslysis shows that a weak
monopole sound source occurs, and at low subsonic flow velocities, this source
generates significant acoustic energy. Comparisons of the theoretical
predictions with available experimental data support this conclusion.

Subject: Transition Noise - The Role of Fluctuating Displacement Thickness

References: See page 22.

Abstract: The role of the fluctuating wall shear stress on the noise gener-
ated by incompressible boundary-layer transition was recently
analyzed [G. C. Lauchle, J. Acoust. Soc. Am. 67, 158-168 (1980)].
The solutions of that analysis suggest that the shear stress
mechanism generates hydrodynamic sound weakly in comparison say
to the sound generated by a fully developed turbulent boundary
layer flow. Because boundary-layer transition is a very unstable
and non-steady flow, we might expect that other acoustic mechanisms
exist. In this paper, we examine one other; namely, that of the
fluctuating boundary layer displacement thickness which is expected
to occur as turbulence bursts are created and convected over the
surface. The analysis shows that a weak monopole sound source
occurs, and at low subsonic flow velocities, this source generates
significant acoustic energy. Comparisons of the theoretical
predictions with available experimental data support this
conclusion.

TABLE OF CONTENTS

LIST OF FIGURES

INTRODUCTION

This author has recently analyzed the role of the fluctuating wall shear stress on the radiated noise due to incompressible boundary-layer transition [1]. In the development of that solution, several types of sources were identified under the assumption of the boundary layer flow being confined to one side of an infinite rigid planar surface. Quadrupoles and octupoles resulted from the fluctuating Reynolds stresses and their images while a longitudinal dipole resulted from the shear stress fluctuations. Under the assumption of low Mach number flow, the dipole was considered to dominate and was hence analyzed in detail. Upon comparing predictions using the shear stress model for the noise with experimental data, rather poor agreement was achieved. Because the computed radiation efficiency was also found to be low, the discrepancy between theory and experiment was not unexpected. That is, the experiment was performed with a buoyant body that supports a substantial area of fully-developed turbulent flow which, based on the magnitude of relative radiation efficiencies, would be expected to dominate the noise spectrum.

Although controversy exists as to whether the transition zone is an important source of hydrodynamic noise, it appears that further analysis and experiment are required in order to resolve the issue. In the tutorial paper by Haddle and Skudrzyk [2], p. 149, the authors state, "...the region where turbulence starts is particularly unstable and intermittent, and must be expected to generate more sound than the rest of the unit." From experiments this author performed in The Garfield Thomas Water Tunnel [3], this statement was partially substantiated;

however, the theory of Ref. [1] does not predict any excessive noise over

that of a turbulent boundary layer alone. Realizing that boundary-layer

transition is a very complicated type of flow, the use of only one mecha-

nism to describe its overall noise production is probably not justified.

The shear stress mechanism certainly contributes, but it may not be the

dominant one.

In this paper we will consider another type of mechanism; one that

gives rise to monopole sound radiation. Its existence is established

through a qualitative look into the physics of intermittent boundary-

layer flow. It is well known from elementary boundary layer theory that

the displacement thickness represents a distance from the wall through

which the potential outer flow is displaced due to the presence of the

boundary layer. In other words, it represents a mass flow deficit.

Thus, if the displacement thickness is known to undergo fluctuations in

time, then one can expect mass flow fluctuations near the surface. These

fluctuations then act on the potential outer flow (acoustic medium) in

much the same way as a vibrating surface acts on its surrounding medium.

The normal velocity of the surface, which can be termed the piston velocity,

defines a boundary condition with which the wave equation may be solved

for the sound pressure. By constructing a model for the displacement

thickness fluctuations that occur within the transition zone, an equivalent

piston velocity is similarly defined. The wave equation is then solved

by straightforward methods such as those used in the study of sound radi-

ation from randomly vibrating structures.

The concept of a displacement effect is not new. It is discussed in

some detail by Laufer, Ffowcs Williams, and Childress [4] in regards to

the noise generated by turbulent boundary layers. The idea was first

proposed by Liepmann, but apparently was never published [4]. As long

as the wave equation forms the basis for the modeling, the results

derived from this approach should be equivalent to those derived from

Lighthill's analogy. The main difference is that the unknown is now

contained within the boundary condition and not within the source terms

of Lighthill's equation.

The analysis presented in this paper is based on the displacement

effect. The power spectrum and radiation efficiency are predicted using

analytical techniques similar to those of Ref. [1]. To help in the veri-

fication of this theory, three examples will be presented in which

experimental data exist.

I. ANALYSIS

Following Ref. [1], we consider the viscous flow of free-stream

velocity u_0 over a flat plate. If a laminar boundary layer begins to

form at the origin of our Cartesian coordinate system, and if the flow

direction is in the x_1-direction, then the flow will ultimately become

nonlinearly unstable at the downstream line $x_1 = x_0$ (see Fig. 1). There

is then a short distance, Δx, over which turbulent "bursts" occur.

Along $x_1 = x_0 + \Delta x$, the flow becomes fully turbulent while for $x_1 < x_0$,

the flow is assumed completely laminar.

Within the source region, $x_0 \leq x_1 \leq x_0 + \Delta x$, the boundary layer

intermittently changes from laminar to turbulent regimes. The bursts of

turbulence usually grow as they convect downstream at some mean convection

velocity, u_c. The locus of a typical burst forms a wedge of apex angle

2α, where we will assume Emmons' [5] result that $\alpha \simeq 9.6°$. Now, at any arbitrary location within the source region, there are going to be instants of time when the boundary-layer flow is laminar while at other instants it will be turbulent. The intermittency factor, $\gamma(x_1)$, is a measure of the percentage of time that the boundary layer is turbulent. Through very carefully performed experiments on a flat plate, Dhawan and Narasimha [6] showed that at x_1 where $0 < \gamma(x_1) < 1$, the mean value of boundary layer displacement thickness is given simply by:

$$<\delta^*> = (1 - \gamma)\ \delta_L^* + \gamma\delta_T^* \quad , \tag{1}$$

where subscript L stands for the laminar flow value and T stands for the corresponding turbulent flow value. We will assume for the laminar flow regimes a Blausius velocity profile; thus, from Schlichting [7]:

$$\delta_L^* = 1.7208\ \frac{\nu}{u_0}\ Re_{x_1}^{1/2} \quad , \tag{2}$$

where ν is the kinematic viscosity of the fluid and Re_{x_1} is the local value of length Reynolds number $(u_0\ x_1/\nu)$. Within the turbulent bursts we will assume a one-seventh power law for the velocity profile, from which [7]:

$$\delta_T^* = 0.04625\ x_1\ Re_{x_1}^{-1/5} \quad . \tag{3}$$

Both Eq. (2) and Eq. (3) were developed under the assumption of a zero pressure gradient, but they may be used with reasonable confidence in flows with mild favorable pressure gradients.

The temporal variation of δ^* through the transition zone is the most important ingredient in the development of the present acoustic theory. No known measurements are available; therefore, we must propose a mathematical model based upon physical intuition. This was the approach used to model the fluctuating wall shear stress in the previous analysis [1]. Realizing that δ^* cannot instantaneously change from a laminar value [Eq. (2)] to a turbulent value [Eq. (3)], we must introduce a time constant, t_i, which mimics the time required for δ^* to change from δ_L^* to δ_T^* (rise time) or visa versa (fall time). For the purposes of the current analysis we will assume the rise time equals the fall time and that during the rise and fall periods, δ^* obeys an exponential dependence with time. Thus, we propose that at a point:

$$\delta^*(t) = [1 - \tilde{I}(t)] \, \delta_L^* + \tilde{I}(t) \, \delta_T^* \quad , \tag{4}$$

where $\tilde{I}(t)$ is a random indicator function as shown in Fig. 2(a).

Following Laufer, et.al. [4], the linearized boundary condition on the acoustic field is

$$v_n = \left(\frac{\partial \phi}{\partial x_2}\right)_{x_2 = 0} = \frac{\partial \delta^*}{\partial t} \quad , \tag{5}$$

where ϕ is the velocity potential of the sound field. From Eq. (4), Eq. (5) becomes

$$v_n = \Delta \delta^* \, \dot{\tilde{I}}(t) \quad , \tag{6}$$

where $\Delta\delta^* \equiv \delta^*_T - \delta^*_L$ and $\dot{I} = \partial I/\partial t$ which is depicted in Fig. 2(b). The velocity, v_n is the equivalent "piston velocity" of the surface due to fluctuations in the boundary layer displacement thickness. The acoustic problem now becomes one of a flexible plane surface of pre-scribed normal velocity, v_n. The solution for the sound field is well known. Crighton [8] gives a concise derivation, finding:

$$p(r,t) = \frac{\rho}{4\pi r} \frac{\partial}{\partial t} \iint_S v_n\left[\underline{n}, \; t - \frac{|\underline{x} - \underline{n}|}{c}\right] d\underline{n} \quad , \tag{7}$$

where p is the acoustic pressure, ρ is the fluid mass density, $r = |\underline{x}|$, c is the sound velocity, and S is the area covered by the sources. Equation (7) shows no angular dependence; hence, the displacement effect creates monopole-type sound radiation. This equation can be simplified somewhat. Consider for the surface a typical length scale, W (Fig. 1), and for the transition zone, length and velocity scales Δx and u_c, respectively. Then, Crighton shows that

$$p(r,t) \simeq \frac{\rho}{4\pi r} \frac{\partial}{\partial t} \iint_S v_n(\underline{n}, \; t - r/c) \; d\underline{n} \tag{8}$$

if and only if $W/c \ll \Delta x/u_c$. In this simplification, the integral may be interpreted as the total instantaneous rate of mass outflow created by the surface.

Substituting for v_n, Eq. (8) takes on the form:

$$p(r,t) \simeq \frac{\rho}{4\pi r} \frac{\partial}{\partial t} \int_0^{\Delta x} \int_{-\infty}^{\infty} \Delta\delta^*(n_1)\dot{I}(n_1,n_3, \; t - r/c) \; dn_1 \; dn_3 \quad , \tag{9}$$

where the origin of our coordinate system has been displaced x_0 units downstream.

A. Power Spectral Density

By definition, the power spectral density function may be derived from the Fourier transform of the autocorrelation function of the radiated acoustic pressure, i.e.,

$$G(r,f) = 2 \int_{-\infty}^{\infty} <p(r,t)\ p(r,t + \tau)>\ e^{i\omega\tau}\ d\tau \quad , \tag{10}$$

where $\omega = 2\pi f$ which is the radian frequency and τ is the delay time associated with the correlation function. We would like to simplify Eq. (9) one step farther by making a parallel flow assumption over the source region. Thus, $\Delta\delta^*(\eta_1)$ is considered independent of η_1 which is certainly plausable when Δx is small. The term $\Delta\delta^*$ may be brought outside the integrals and evaluated at some average value of x_1, e.g., $\bar{x}_1 = x_0 + \Delta x/2$.

Equation (10) is now of the form:

$$G(r,f) \simeq \frac{\rho^2 (\Delta\delta^*)^2 \omega^2}{8\pi^2 r^2} \iiiint\int <\ddot{I}(\eta_1,\eta_3,t - r/c)$$

$$\cdot\ \ddot{I}(\eta_1 + \xi_1,\ \eta_3 + \xi_3,\ t - r/c + \tau)>e^{i\omega\tau}\ d\eta_1\ d\eta_3\ d\xi_1\ d\xi_3\ d\tau,$$

where the ω^2 arises from the Fourier transform of the second time derivative of the space/time correlation function of $\overset{\ast}{\mathbf{I}}$. As in Ref. [1], we assume $\overset{\ast}{\mathbf{I}}$ to be stationary in time, homogeneous in x_3, and non-homogeneous in x_1. Then,

$$G(r,f) \simeq \frac{\rho^2 (\Delta \delta^*)^2 \omega^2}{8\pi^2 r^2} \iiiint\!\!\int \langle \overset{\ast}{\mathbf{I}}(\eta_1, 0, 0)$$

$$\cdot\; \overset{\ast}{\mathbf{I}}(\eta_1 + \xi_1,\; \xi_3,\; \tau)\rangle\; e^{i\omega\tau}\; d\eta_1\; d\eta_3\; d\xi_1\; d\xi_3\; d\tau \quad . \tag{11}$$

A very useful theorem, given by Stratonovich [9], allows us to rewrite Eq. (11) in terms of the correlation function for a random sequence of delta functions, $\overset{\bullet}{\mathbf{I}}(t)$ [Fig. 3(a)] and a "frequency depression factor," $|J(i\omega)|^2$. The quantity $J(i\omega)$ is simply the Fourier transform of an individual pulse shape of Fig. 2(b). Using this theorem, Eq. (11) is identical to:

$$G(r,f) \simeq \frac{\rho^2 (\Delta \delta^*)^2 \omega^2}{8\pi^2 r^2}\; |J(i\omega)|^2 \iiiint\!\!\int \langle \overset{\bullet\bullet}{\mathbf{I}}\mathbf{I}'\rangle\; e^{i\omega\tau}\; d\underline{\eta}\; d\underline{\xi}\; d\tau \quad ,$$

where $\langle \overset{\bullet\bullet}{\mathbf{I}}\mathbf{I}'\rangle$ is shorthand notation for the space/time correlation function. Again noting [1] that $\langle \overset{\bullet\bullet}{\mathbf{I}}\mathbf{I}'\rangle = -\partial^2 \langle \mathbf{I}\mathbf{I}'\rangle/\partial\tau^2$, Eq. (11) becomes:

$$G(r,f) \simeq \frac{\rho^2 (\Delta \delta^*)^2 \omega^4}{8\pi^2 r^2}\; |J(i\omega)|^2 \iiiint\!\!\int \langle \mathbf{I}(\eta_1, 0, 0)$$

$$\cdot\; \mathbf{I}(\eta_1 + \xi_1,\; \xi_3,\; \tau)\rangle\; e^{i\omega\tau}\; d\eta_1\; d\eta_3\; d\xi_1\; d\xi_3\; d\tau \quad , \tag{12}$$

where $I(t)$ is the "ideal" indicator function of Fig. 3(b). The frequency depression factor is easily calculated:

$$J(i\omega) = \frac{1}{2} V_0 \int_{-\infty}^{\infty} e^{-|t|/t_i} e^{i\omega t} dt = V_0 \int_0^{\infty} e^{-t/t_i} e^{i\omega t} dt \quad . \quad (13)$$

The constant V_0 is determined from the condition [9] that $J(0) = 1$. We find $V_0 = t_i^{-1}$, from which Eq. (13) becomes:

$$J(i\omega) = (1 - i\omega t_i)^{-1} \quad ,$$

and

$$|J(i\omega)|^2 = [1 + (\omega t_i)^2]^{-1} \quad . \quad (14)$$

The integrals of Eq. (12) are now identical to those treated in Eq. (23) of Ref. [1]. We will not repeat the details here, but point out that $<II'>$ was assumed separable, i.e.,

$$<II'> = R_1(\eta_1, \xi_1, \tau) R_2(\eta_1, \xi_3) \quad , \quad (15)$$

where

$$\int_{-\infty}^{\infty} R_2(\eta_1, \xi_3) d\xi_3 \simeq 3 \eta_1 \tan\alpha \quad , \quad (16)$$

and

$$R_1(\eta_1, \xi_1, \tau) \simeq \gamma(\eta_1) \exp(-\alpha^*|\xi_1|) \exp(-2N|\tau - \xi_1/u_c|) \quad (17)$$

with

$$\alpha^* \simeq (1 + 83.35 \, z^8)/\Delta x \quad (18)$$

$$\gamma(z) \simeq 1 - e^{-4.185 \, z^2} \quad (19)$$

$$N(z) \simeq 1.272 \ (u_0/\Delta x) z e^{-4.185 \ z^2} \tag{20}$$

and

$$z = \eta_1/\Delta x \quad . \tag{21}$$

The distributions for the intermittency factor and burst frequency given in Eqs. (19) and (20), respectively are taken from Farabee, et. al. [10].

The power spectral density of the far-field acoustic pressure radiated per unit spanwise width of boundary-layer transition becomes:

$$\frac{\partial G(r,f)}{\partial x_3} \simeq \frac{\rho^2 (\Delta \delta^*)^2 \ u_0 \ u_c^2}{8\pi^2 \ r^2} \ F^*(k_c \Delta x, \ \alpha^* \Delta x, \ u_c t_i/\Delta x, \ u_c/u_0) \quad , \tag{22}$$

where

$$F^* = \frac{(k_c \Delta x)^2 \ F(k_c \Delta x, \ \alpha^* \Delta x, \ u_c/u_0)}{[1 + (k_c \Delta x)^2 (u_c t_i/\Delta x)^2]} \quad , \tag{23}$$

$$F(k_c \Delta x, \alpha^* \Delta x, u_c/u_0) = (k_c \Delta x)^2 \int_0^1 \frac{1.272 z^2 (1 - e^{-4.185 z^2}) e^{-4.185 z^2}}{\left[6.472 \left| \frac{u_0}{u_c} \right|^2 z^2 e^{-8.37 z^2} + (k_c \Delta x)^2 \right] [(\alpha^* \Delta x)^2 + (k_c \Delta x)^2]^{1/2}}$$

$$\cdot \left\{ \frac{2\alpha^* \Delta x}{[(\alpha^* \Delta x)^2 + (k_c \Delta x)^2]^{1/2}} - e^{-\alpha^* \Delta x z} \sin(k_c \Delta x z - \phi) + e^{-\alpha^* \Delta x (1-z)} \sin[k_c \Delta x (1-z) - \phi] \right\} dz, \tag{24}$$

with

$$\phi = \tan^{-1} (\alpha^* \Delta x / k_c \Delta x) \quad , \quad \text{and} \ k_c = \omega/u_c \quad .$$

Equation (23) has been integrated numerically by Simpson's rule. Typical results of this computation are presented in Figs. 4 and 5. It is seen from these figures that the magnitude of the high-frequency portion of the spectrum depends significantly on the value of the nondimensional rise time, $u_c t_i / \Delta x$. At very low values of $k_c \Delta x$, the spectral levels rise at 12 dB/octave and are essentially independent of $u_c t_i / \Delta x$. For $k_c \Delta x \gg 1$, the spectral levels roll off at 6 dB/octave. The frequency of the peak in the spectrum depends upon $u_c t_i / \Delta x$.

As noted in Figs. 4 and 5, the selected range for the nondimensional rise time is between 0.05 and 1.35. This range was established through the following dimensional reasoning. We expect that t_i scales with the length $\Delta \delta^*$ and with the velocities very near and normal to the surface; these velocities scale with the friction velocity, u_*. Thus, $t_i \sim \Delta \delta^* / u_*$. Letting $u_* \simeq u_0/30$ and $u_c \simeq 0.7\, u_0$, we conclude that

$$\frac{u_c t_i}{\Delta x} \sim 20\, \frac{\Delta \delta^*}{\Delta x} \quad . \tag{25}$$

For typical values of $\Delta \delta^*$ and Δx as will be discussed in SECTION II, the above relationship suggests that $0.05 \leq u_c t_i / \Delta x \leq 1.35$.

B. Radiation Efficiency

If we denote the right-hand side of Eq. (22) by $\langle p_0^2 \rangle$, then the power radiated per unit spanwise width is given by:

$$N_a = \int_0^\infty \frac{\langle p_0^2 \rangle}{\rho c}\, d\omega \int_0^{2\pi} d\theta \int_0^\pi r^2 \sin\theta\, d\theta \quad . \tag{26}$$

substituting for $<p_0{}^2>$, we find:

$$N_a \simeq \frac{\rho(\Delta\delta^*)^2 u_0 u_c{}^3 \overline{F^*}}{2 \pi c \Delta x} \quad , \tag{27}$$

where

$$\overline{F^*} = \int_0^\infty F^* \, d(k_c \Delta x) \quad . \tag{28}$$

The numerical value of $\overline{F^*}$ depends upon $u_c t_i/\Delta x$, where typical values are tabulated on Figs. 4 and 5. The radiation efficiency is defined as the ratio of acoustic power to hydrodynamic power generated by the source region. It was shown by Lauchle [1] that the hydrodynamic power for transitional flow is given by:

$$N_h \simeq 0.572 \, u_0 \, \Delta x \, \sigma \tag{29}$$

where $\sigma \equiv \tau_T(x_0) - \tau_L(x_0)$ which is the difference between the turbulent and laminar values of wall shear stress at the beginning of intermittent flow. Dividing Eq. (28) by Eq. (29), the transition zone radiation efficiency results:

$$\eta_{tr} \simeq 0.278 \, \frac{\rho u_c{}^3}{c\sigma} \left(\frac{\Delta\delta^*}{\Delta x}\right)^2 \overline{F^*} \quad . \tag{30}$$

Noting that $\Delta\delta^*/\Delta x$ is only weakly dependent on u_0 and that $\sigma \sim \rho u_0{}^2$, $\eta_{tr} \sim u_0/c$ which is to be expected for a monopole source.

In analyzing the role of shear stress fluctuations on transition

noise [1], the computed radiation efficiency was compared with that of

a fully developed turbulent boundary layer flow [11]. Repeating that

comparison here, for the case of a fluctuating displacement thickness

mechanism, we find:

$$\frac{\eta_{tr}}{\eta_{TBL}} \simeq 1.48 \left[\frac{\rho c \; \Delta\delta^*}{\Delta x}\right]^2 \frac{u_c^3 \; \overline{F^*}}{\sigma \, \tau_T \, u_0} \quad , \tag{31}$$

where $\eta_{TBL} \simeq 0.188 \, \tau_T \, u_0/\rho c^3$. Noting that $u_c \sim u_0$, and that $\sigma \, \tau_T \sim (\rho \, u_0^2)^2$,

Eq. (31) shows that $\eta_{tr} \sim \eta_{TBL}/M^2$, where M is the free-stream Mach number.

Through use of an emperical relation for Δx derived by Chen and Thyson [12],

i.e.,

$$\Delta x \simeq 60 \; x_0 \; Re_{x_0}^{-1/3} \quad , \tag{32}$$

where Re_{x_0} is the transition point Reynolds number, and through use of

Eqs. (2) and (3), it is easy to show that

$$\Delta\delta^*/\Delta x \simeq 7.708 \times 10^{-4} \; Re_{x_0}^{2/15} - 2.868 \times 10^{-2} \; Re_{x_0}^{-1/2} \quad . \tag{33}$$

Also, from Ref. [1],

$$\sigma \, \tau_T \simeq \left[0.0288 \; \rho \; u_0^2 \; Re_{x_0}^{-1/5}\right]^2 \left[1 - 11.53 \; Re_{x_0}^{-3/10}\right] \quad . \tag{34}$$

Thus, η_{tr}/η_{TBL} depends only upon Re_{x_0}, M, and $u_c t_i/\Delta x$. Figure 6 shows

the dependence of η_{tr}/η_{TBL} on M for a range of rise times and with

$Re_{x_0} = 4 \times 10^6$ and $u_c = 0.8 u_0$.

Some caution should be exercised when interpreting Fig. 6. The

ratio of radiation efficiencies presented here assumes equal source areas.

In practice, say for a body of revolution moving through water, the area

of transition is $\Delta x W$ while the area of fully-developed turbulent flow is

of the same order as the body surface area, A_b. Clearly, $A_b \gg \Delta x W$ which

means that a measured radiated noise spectrum may certainly contain

significant contributions from the fully-developed turbulent flow.

II. EXAMPLES

By way of numerical examples, we will consider those cases in which

flow noise was measured experimentally under anechoic or near-anechoic

conditions. It is pointed out from the outset that for each of these

examples, the experimentalists' goal was to measure the overall flow

noise of the vehicle or fixture at different points in space. We there-

fore select those measurement points which, based on our physical insight,

would appear to be most influenced by the noise generated by the transition

zone. It is further pointed out that many of the hydrodynamic parameters

that characterize the transition zone flow are not available for the

examples discussed below. We have therefore estimated them using theoretical

considerations. The most significant unknown is the rise time, t_i. Because

there are no definitive measurements of this time constant, we have elected

to use the dimensional analysis that led to Eq. (25).

A. Case 1: Flat Plate in Air

DeMetz and Casarella [13] performed extensive measurements of the fluctuating pressures that occur within the transition region of a large flat plate operating in an anechoic wind tunnel. Of their data, we select a condition where the microphone was located within the laminar boundary layer so that its response would be due only to the noise generated by the downstream unsteady flow. A spectrum of this noise is presented in Fig. B-3 of Ref. [13]. Here, Re_{x_0} = 7.5 x 10^6 and the measurement took place at Re_{x_1} = 4.758 x 10^6. Based on the difference of these two Reynolds numbers, r can be estimated to be 1.55 m. The width of the plate, W, is 2.44 m, which is multiplied by Eq. (22) in order to obtain the radiated noise due to the entire width of transitional flow. Now, the total plate length is 4.34 m and x_0 = 4.26 m; therefore $\Delta x \simeq$ 76 mm. In other words, transition has occurred right before the trailing edge and the data should therefore be uncontaminated by any noise due to fully-developed turbulent flow [Eq. (32) predicts Δx > 76 mm].

Assuming u_c/u_0 = 0.8, the comparison of our prediction with the experimental spectrum is shown in Fig. 7. DeMetz, et. al. [13] attribute the high energy levels between 5 and 10 kHz as being due to pinhole microphone cavity resonance and plate vibration. Aside from this band, the data compare quite favorably with the present model using $u_c t_1/\Delta x$ = 0.15. Also shown on Fig. 7 is a prediction for the shear stress contribution to the transition zone noise [1]. Clearly, the fluctuating displacement thickness mechanism appears to dominate.

B. Case 2: Buoyant Body in Water

Haddle and Skudrzyk [2] present flow noise spectra measured both on

and far away from a buoyantly-propelled axisymmetric body with a hemi-

spherical nose. Because the terminal velocity is quite high (30-37 knots),

it is assumed that transition occurs on the 0.48 m diameter body before

the laminar separation point. We assume transition occurs at the minimum

pressure point which is predicted to be at $x_0 \simeq 0.32$ m [14]. Thus, for

the 37 knot condition, $Re_{x_0} \simeq 6.27 \times 10^6$ which assumes 21°C fresh water.

The length W is calculated from the circumference of the body at x_0.

Hydrophone no. 7 which is located at a 45° arc from the stagnation point

is selected for the first comparison. The estimated point of transition

is 0.13 m downstream from this hydrophone (thus, r = 0.13 m).

The spectrum measured by hydrophone no. 7 is presented in Fig. 17

of Ref. [2]. We repeat it here in Fig. 8 along with the transition zone

noise predictions for both mechanisms. Again rather good agreement is

achieved for the noise mechanism addressed in this paper. It is noted,

however, that the experimental spectrum rolls off slightly faster than

the predictions. This may be due to a water-borne diffraction loss which

was discussed in some detail by Lauchle [3].

Haddle and Skudrzyk also measured the far-field noise of the buoyant

unit with a distant hydrophone array, e.g., Fig. 19 of Ref. [2]. The

reference distance is the radius of a sphere whose area is the same as

the area of the vehicle, i.e., r = 0.73 m. This run was performed at

30 knots, hence, $Re_{x_0} \simeq 4.97 \times 10^6$. A comparison of our predictions with

the experimental spectrum is shown in Fig. 9. The shear stress contribution

[1] is not shown because its directivity function would predict a null at

the beam aspect angle. It is of interest to note that $\Delta\delta^*$ is calculated

to be 0.43 mm for these experiments and Δx was estimated to be 61 mm.

Equation (25) then suggests that $u_c t_i/\Delta x \simeq 0.14$ which agrees to within a

factor of three of that value used for the prediction which fits the data

the best.

III. CONCLUSIONS

In this paper we have analyzed the role of a fluctuating displacement

thickness on the noise generated by incompressible boundary-layer transition.

In essence, the analytical methods parallel those of an earlier analysis

in which the role of a fluctuating shear stress was addressed [1]. Based

on numerical calculations of the power spectral density and on the relative

magnitudes of the radiation efficiency, the mechanism treated in the present

paper is found to be much more productive as a noise source than is the

shear stress mechanism. The fluctuating displacement thickness effect

gives rise to a monopole-type of sound radiation. The spectrum of the

radiated noise was found to rise at 12 dB/octave, level off, and then fall

off at 6 dB/octave.

The frequency at which the spectrum peaks is not easily defined

because it depends upon a characteristic time, t_i, associated with the

growth of the turbulent boundary layer in a turbulent burst. This time

models the time required for the laminar value of the boundary layer

displacement thickness to change to a turbulent value and visa versa.

The way in which we incorporated t_i into the noise analysis is heuristic.

We assumed that the displacement thickness grows from a laminar value to

a turbulent value according to an exponential time variation and that the

process is symmetrical. There is no experimental evidence that this is

true (or for that matter, any other functional form.) Based on the

comparisons of this theory with experimental data, particularly those of

Case 1, it appears that these assumptions may be realistic.

A basic problem to be resolved deals with the measurement of t_i.

According to Laufer, et. al. [4], $\delta^*(t)$ can, in principle, be measured

in a laboratory frame of reference by performing simultaneous measurements

of the fluctuating velocity and pressure and their correlation through

the boundary layer. One then couples these data with a first order partial

differential equation for δ^* derived by integrating the non-steady

continuity equation across the boundary layer. If this procedure can

be demonstrated, then it is conceivable that t_i can also be measured.

Such measurements, to this author's knowledge, have never been carried

out. Perhaps the findings presented in this paper may provide the impetus

required for future experimental investigations of this type.

REFERENCES

1. G. C. Lauchle, "On the Radiated Noise due to Boundary-Layer Transition,"
    J. Acoust. Soc. Am. 67, 158-168 (1980).

2. G. P. Haddle and E. J. Skudrzyk, "The Physics of Flow Noise," J.
    Acoust. Soc. Am. 46, 130-157 (1969).

3. G. C. Lauchle, "Noise Generated by Axisymmetric Turbulent Boundary-
    Layer Flow," J. Acoust. Soc. Am. 61, 694-702 (1977).

4. J. Laufer, J. E. Ffowcs Williams, and S. Childress, "Mechanism of
    Noise Generation in the Turbulent Boundary Layer," AGARDograph 90
    (1964).

5. H. W. Emmons, "The Laminar-Turbulent Transition in a Boundary Layer -
    Part I," J. Aero. Sci. 18, 490-498 (1951).

6. S. Dhawan and R. Narasimha, "Some Properties of Boundary Layer Flow
    During the Transition from Laminar to Turbulent Motion," J. Fluid
    Mech. 3, 418-436 (1958).

7. H. Schlichting, Boundary-Layer Theory (McGraw Hill, New York, 1968),
    6th ed., pp. 130, 599.

8. D. G. Crighton, "Basic Principles of Aerodynamic Noise Generation,"
    Prog. Aerosp. Sci. 16, 31-96 (1975).

9. R. L. Stratonovich, Topics in the Theory of Random Noise, Volume I
    (Gordon Breach Science Publ., New York, 1963), p. 157.

10. T. M. Farabee, M. J. Casarella, and F. C. DeMetz, "Source Distribution
    of Turbulent Bursts During Natural Transition," David W. Taylor Naval
    Ship Research and Development Center Report SAD-89E-1942, August 1974.

11. C. K. W. Tam, "Intensity, Spectrum, and Directivity of Turbulent

     Boundary Layer Noise," J. Acoust. Soc. Am. 57, 24-34 (1975).

12. K. K. Chen and N. A. Thyson, "Extension of Emmons' Spot Theory to

     Flows on Blunt Bodies, AIAA J. 9, 821-825 (1971).

13. F. C. DeMetz and M. J. Casarella, "An Experimental Study of the

     Intermittent Properties of the Boundary Layer Pressure Field During

     Transition on a Flat Plate," David W. Taylor Naval Ship Research and

     Development Center Report 4140, AD-775-299 (November 1973).

14. These distances are arc lengths originating at the stagnation point.
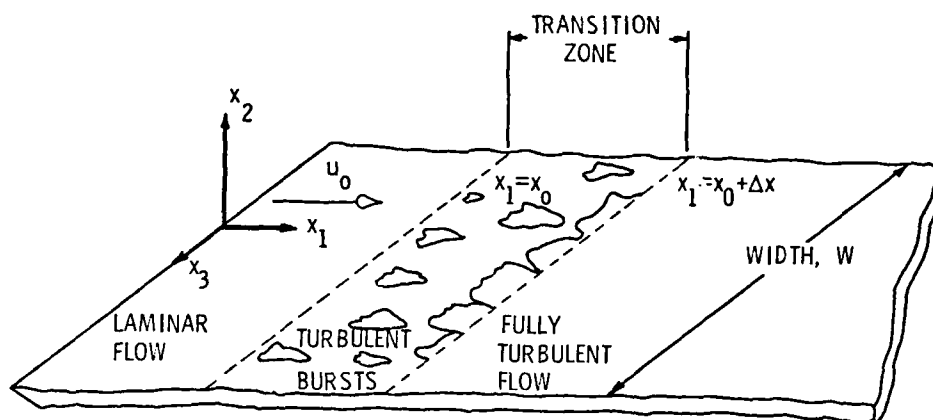
Fig. 1. Schematic representation of the transition from laminar-to-turbulent flow on a flat plate.
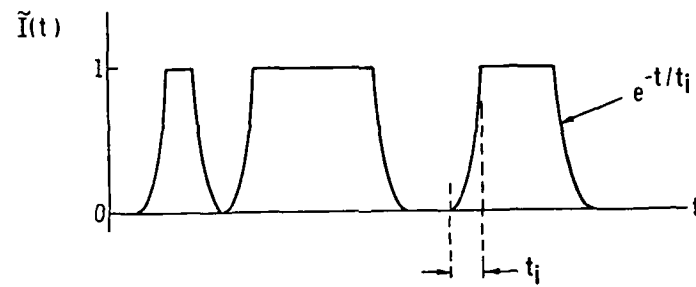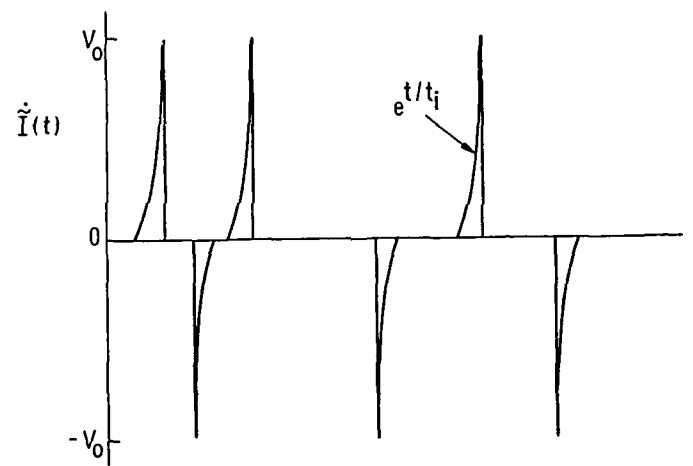
Fig. 2. The indicator function (a) and its first time derivative (b) which is used to model the random variation in displacement thickness during transition.
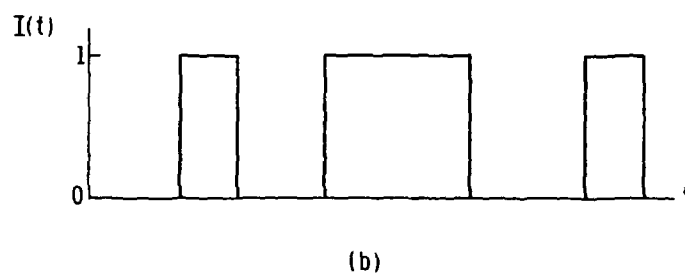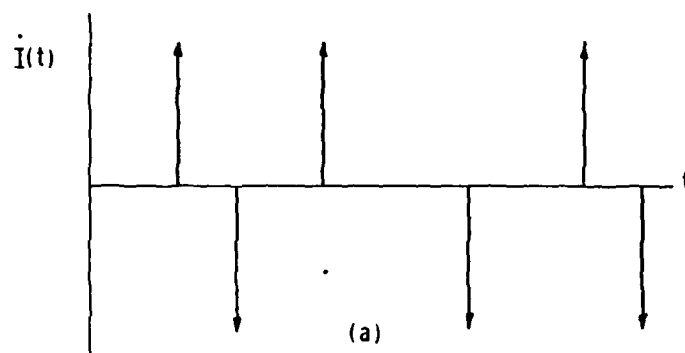
Fig. 3.   The idealistic point process (a) and the ideal indicator
function (b).

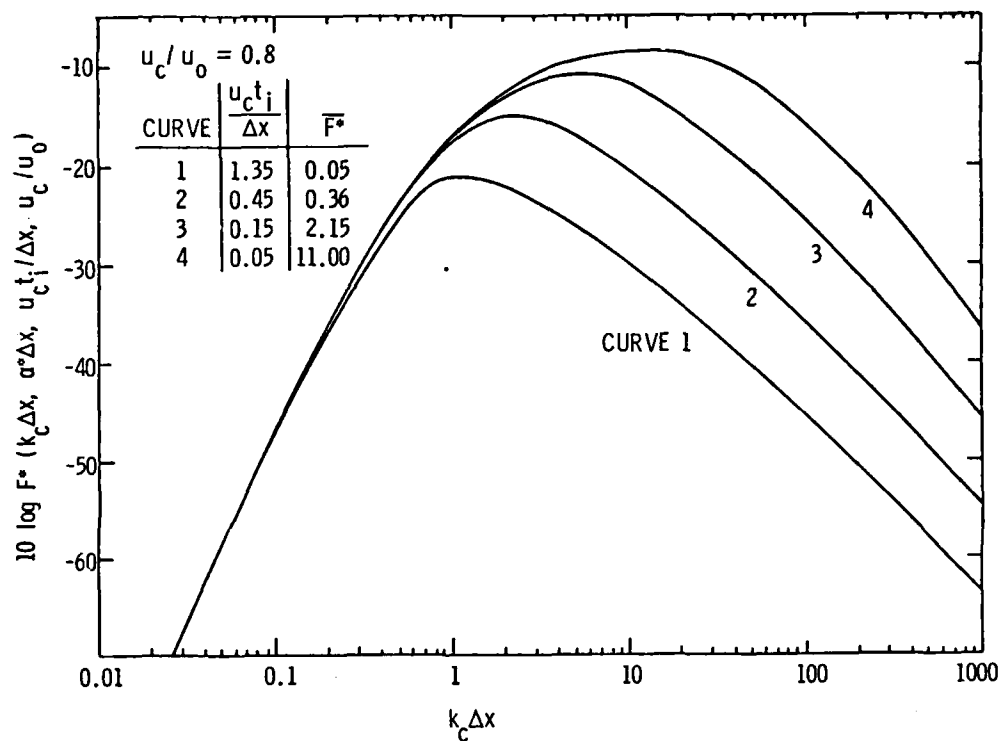Fig. 4. Non-dimensional power spectral density function of Eq. (23) for $u_c = 0.8\ u_0$.
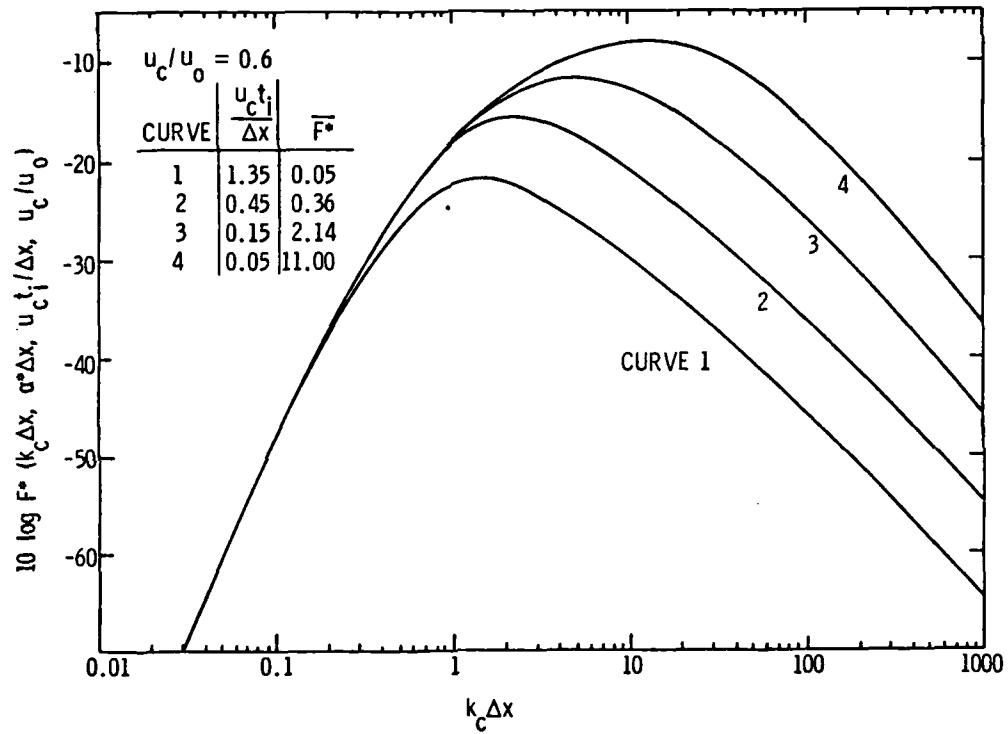
Fig. 5. Non-dimensional power spectral density function of Eq. (23) for
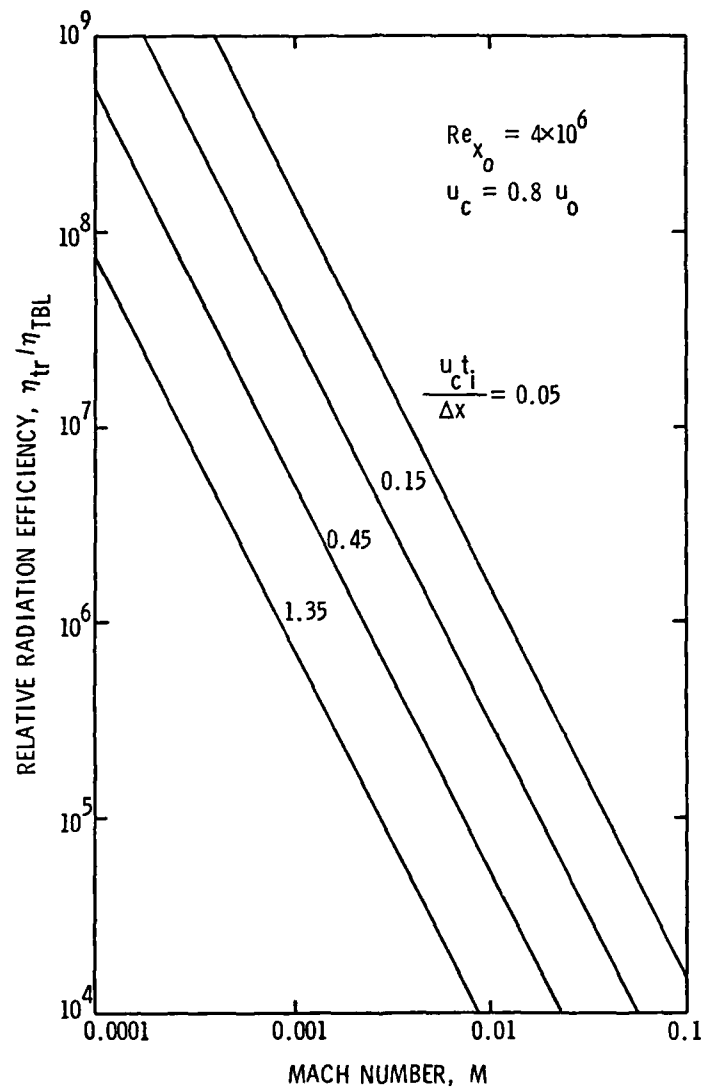
$u_c = 0.6 \ u_0$.

Fig. 6. Relative radiation efficiency, η_{tr}/η_{TBL}, expressed as a function of Mach number.
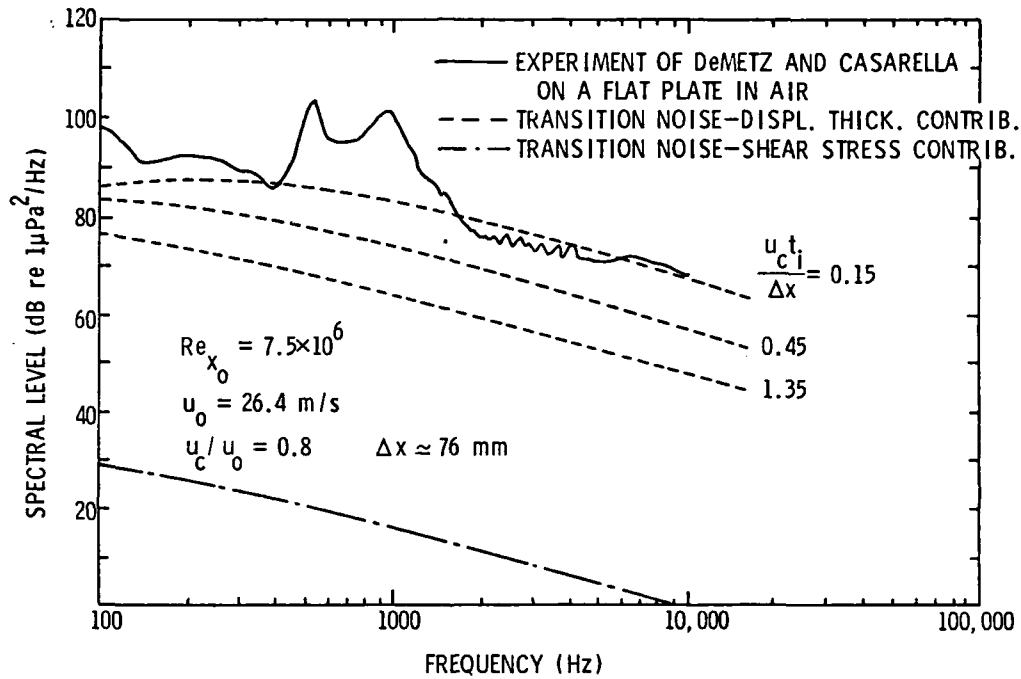
Fig. 7. Comparison of the theory with an experimental spectrum measured
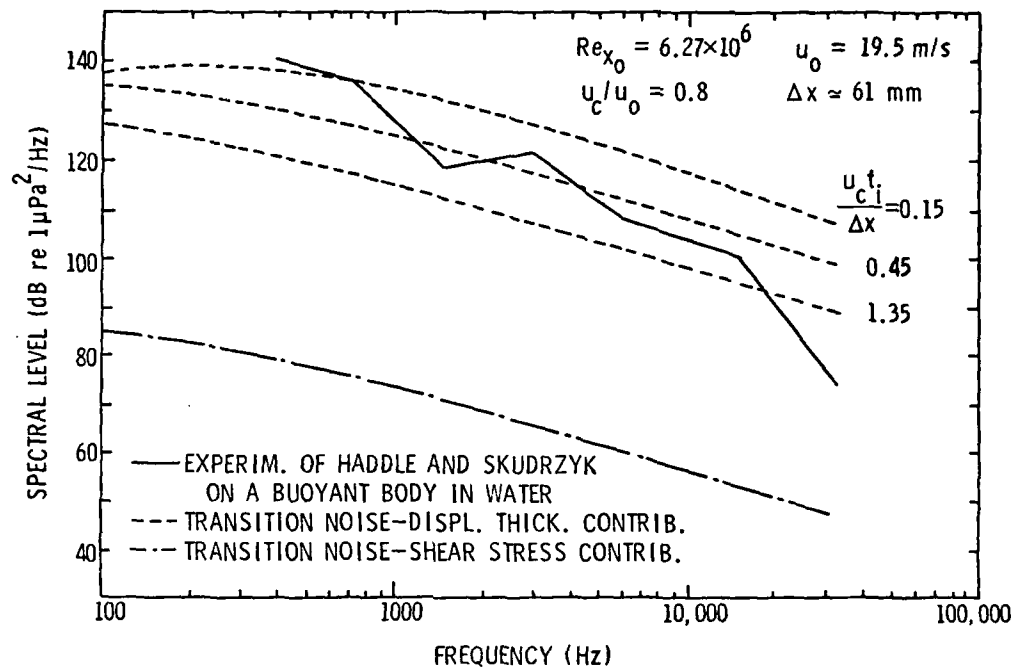on a flat plate by DeMetz and Casarella [13].

Fig. 8. Comparison of the theory with an experimental spectrum measured on the surface of a buoyantly - propelled vehicle by Haddle and Skudrzyk [2].
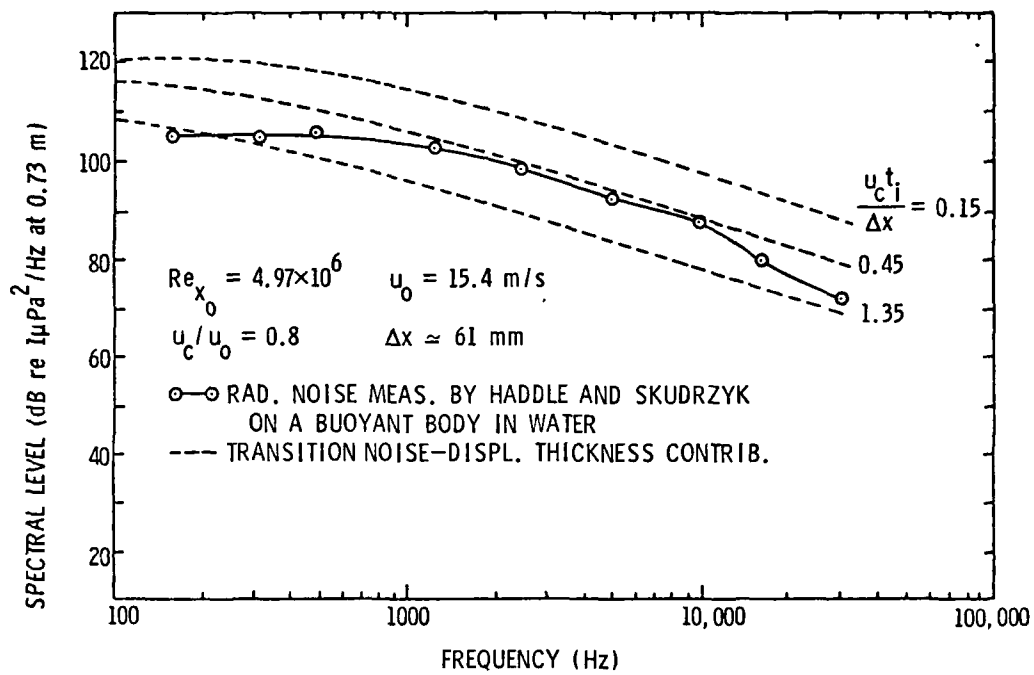
Fig. 9. Comparison of the theory with an experimental spectrum measured far away from the rising buoyant body of Haddle and Skudrzyk [2].

Commander
Naval Sea Systems Command
Department of the Navy
Washington, DC 20362
Attn: Library
   Code NSEA-09G32
(Copies No. 1 and 2)

Naval Sea Systems Command
Attn: E. G. Liszka
   Code NSEA-63R1
(Copy No. 3)

Naval Sea Systems Command
Attn: F. Romano
   Code NSEA-63R
(Copy No. 4)

Naval Sea Systems Command
Attn: T. E. Peirce
   Code NSEA-63R-31
(Copy No. 5)

Naval Sea Systems Command
Attn: J. G. Juergens
   Code NSEA-05H
(Copy No. 6)

Naval Sea Systems Command
Attn: H. C. Claybourne
   Code NSEA-05H
(Copy No. 7)

Naval Sea Systems Command
Attn: A. R. Paladino
   Code NSEA-05H1
(Copy No. 8)

Naval Sea Systems Command
Attn: C. C. Taylor
   Code NSEA-05H
(Copy No. 9)

Naval Sea Systems Command
Attn: D. L. Creed
   Code NSEA-00311
(Copy No. 10)

Naval Sea Systems Command
Attn: W. L. Louis
   Code NSEA-32132
(Copy No. 11)

Naval Sea Systems Command
Attn: F. J. Welling
   Code NSEA-521
(Copy No. 12)

Commanding Officer
Naval Underwater Systems Center
Newport, RI 02840
Attn: C. N. Pryor
   Code 01
(Copy No. 13)

Naval Underwater Systems Center
Attn: D. Goodrich
   Code 36315
(Copy No. 14)

Naval Underwater Systems Center
Attn: R. J. Kittredge
   Code 36313
(Copy No. 15)

Naval Underwater Systems Center
Attn: J. Miguel
   Code 36315
(Copy No. 16)

Naval Underwater Systems Center
Attn: B. J. Myers
   Code 36311
(Copy No. 17)

Naval Underwater Systems Center
Attn: R. H. Nadolink
   Code 36315
(Copy No. 18)

Naval Underwater Systems Center
Attn: D. A. Quadrini
   Code 36314
(Copy No. 19)

Naval Underwater Systems Center
Attn: E. J. Sullivan
   Code 36311
(Copy No. 20)

Naval Underwater Systems Center
Attn: R. Trainor
   Code 36314
(Copy No. 21)

Naval Underwater Systems Center
Attn: Library
   Code 54
(Copy No. 22)

Naval Ocean Systems Center
San Diego, CA 92152
Attn: M. M. Reischman
   Code 2542
(Copy No. 23)

DISTRIBUTION LIST FOR UNCLASSIFIED TM 80-41 by G. C. Lauchle, dated 27 March 1980

Commander
David W. Taylor Naval Ship R&D Center
Department of the Navy
Bethesda, MD 20084
Attn: Code 1505
(Copy No. 24)

David W. Taylor Naval Ship R&D Center
Attn: J. H. McCarthy
        Code 1552
(Copy No. 25)

David W. Taylor Naval Ship R&D Center
Attn: T. E. Brockett
        Code 1544
(Copy No. 26)

David W. Taylor Naval Ship R&D Center
Attn: M. M. Sevik
        Code 19
(Copy No. 27)

David W. Taylor Naval Ship R&D Center
Attn: W. K. Blake
        Code 1942
(Copy No. 28)

David W. Taylor Naval Ship R&D Center
Attn: T. M. Farabee
        Code 1942
(Copy No. 29)

David W. Taylor Naval Ship R&D Center
Attn: M. J. Casarella
        Code 1942
(Copy No. 30)

Officer-in-Charge
David W. Taylor Naval Ship R&D Center
Department of the Navy
Annapolis Laboratory
Annapolis, MD 21402
Attn: J. G. Stricker
        Code 2721
(Copy No. 31)

Commander
Naval Surface Weapon Center
Silver Spring, MD 20910
Attn: G. C. Gaunaurd
        Code R-31
(Copy No. 32)

Naval Surface Weapon Center
Attn: Library
(Copy No. 33)

Office of Naval Research
Department of the Navy
800 N. Quincy Street
Arlington, VA 22217
Attn: H. Fitzpatrick
        Code 438
(Copy No. 34)

Office of Naval Research
Attn: R. D. Cooper
        Code 438
(Copy No. 35)

Naval Research Laboratory
Attn: R. J. Hansen
        Code 20375
(Copy No. 36)

Defense Technical Information Center
5010 Duke Street
Cameron Station
Alexandria, VA 22314
(Copies No. 37 - 48)

National Bureau of Standards
Aerodynamics Section
Washington, DC 20234
Attn: P. S. Klebanoff
(Copy No. 49)

Rand Corporation
1700 Main Street
Santa Monica, CA 90406
Attn: C. Gazley
(Copy No. 50)

Jet Propulsion Laboratory
4800 Oak Grove Drive
Pasadena, CA 91108
Attn: L. M. Mack
(Copy No. 51)

Hersh Acoustical Engineering
9545 Cozycroft Avenue
Chatsworth, CA 91311
Attn: A. Hersh
(Copy No. 52)

Dynamics Technology, Inc.
3838 Carson Street, Suite 110
Torrance, CA 90503
Attn: W. N. Haigh
(Copy No. 53)

Dynamics Technology, Inc.
Attn: D. R. S. Ko
(Copy No. 54)

Bolt Beranek and Newman
50 Moulton Street
Cambridge, MA 20136
Attn: N. Brown
(Copy No. 55)

Bolt Beranek and Newman
Attn: D. Chase
(Copy No. 56)

Bolt Beranek and Newman
Attn: K. L. Chandiramani
(Copy No. 57)

Kentex International, Inc.
2054 University Avenue - #301
Berkeley, CA 94704
Attn: S. Yang
(Copy No. 58)

Bell Laboratories
Whippany Road
Whippany, NJ 07981
Attn: J. G. Berryman
(Copy No. 59)

Massachusetts Institute of Technology
77 Massachusetts Avenue
Cambridge, MA 02139
Attn: Prof. Patrick Leehey
      Department of Ocean Engineering
      Room 5-222
(Copy No. 60)

Massachusetts Institute of Technology
Attn: M. T. Landahl
(Copy No. 61)

Cornell University
Sibley School of Mechanical and
    Aeronautical Engineering
Upson Hall
Ithaca, NY 14850
Attn: Dr. J. L. Lumley
(Copy No. 62)

University of Minnesota
St. Anthony Falls Hydraulic Laboratory
Mississippi River at 3rd Avenue S.E.
Minneapolis, MN 55414
Attn: R. E. A. Arndt
(Copy No. 63)

University of Minnesota
Attn: L. G. Straub Memorial Library
(Copy No. 64)

University of Leeds
Department of Applied Mathematical Studies
Leeds LS29JT, England
Attn: Dr. D. G. Crighton
(Copy No. 65)

A. G. Fabula
5497 Coral Reef Avenue
La Jolla, CA 92037
(Copy No. 66)

O. F. Griffith
Department of Physics
University of New Orleans
Lake Front
New Orleans, LA 70122
(Copy No. 67)

Mark V. Morkovin
Department of Mech. and Aerosp. Engr.
Illinois Inst. of Tech.
3300 S. Federal Street
Chicago, Illinois 60616
(Copy No. 68)

William K. George
SUNY at Buffalo
Department of Mechanical Engineering
Parker Engr. Building
Buffalo, NY 14214
(Copy No. 69)

L. Maestrello
MS 460
NASA Langley Research Center
Hampton, VA 23665
(Copy No. 70)

R. F. Mons
Westinghouse Electric Corp.
P.O. Box 1458
Annapolis, MD 21404
(Copy No. 71)

Applied Research Laboratory
The Pennsylvania State University
Post Office Box 30
State College, PA 16801
Attn: B. R. Parkin
(Copy No. 72)

Applied Research Laboratory
Attn: E. J. Skudrzyk
(Copy No. 73)

DISTRIBUTION LIST FOR UNCLASSIFIED TM 80-41 by G. C. Lauchle, dated 27 March 1980

Applied Research Laboratory
Attn: G. H. Hoffman
(Copy No. 74)

Applied Research Laboratory
Attn: G. C. Lauchle
(Copy No. 75)

Applied Research Laboratory
Attn: GTWT File
(Copy No. 76)